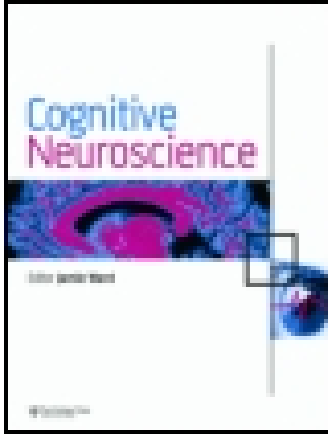


This article was downloaded by: [Universitaetsbibliothek Bonn], [Leila Chaieb]

On: 24 June 2015, At: 01:18

Publisher: Routledge

Informa Ltd Registered in England and Wales Registered Number: 1072954 Registered office: Mortimer House, 37-41 Mortimer Street, London W1T 3JH, UK



Cognitive Neuroscience

Publication details, including instructions for authors and subscription information:
<http://www.tandfonline.com/loi/pcns20>

Theta-gamma phase-phase coupling during working memory maintenance in the human hippocampus

Leila Chaieb^a, Marcin Leszczynski^a, Nikolai Axmacher^{bc}, Marlene Höhne^a, Christian E. Elger^{ad} & Juergen Fell^a

^a Department of Epileptology, University of Bonn, Bonn, Germany

^b Department of Neuropsychology, Institute of Cognitive Neuroscience, Ruhr-University Bochum, Bochum, Germany

^c German Center for Neurodegenerative Diseases, Bonn, Germany

^d Life and Brain GmbH, Bonn, Germany

Published online: 23 Jun 2015.



[Click for updates](#)

To cite this article: Leila Chaieb, Marcin Leszczynski, Nikolai Axmacher, Marlene Höhne, Christian E. Elger & Juergen Fell (2015): Theta-gamma phase-phase coupling during working memory maintenance in the human hippocampus, Cognitive Neuroscience, DOI: [10.1080/17588928.2015.1058254](https://doi.org/10.1080/17588928.2015.1058254)

To link to this article: <http://dx.doi.org/10.1080/17588928.2015.1058254>

PLEASE SCROLL DOWN FOR ARTICLE

Taylor & Francis makes every effort to ensure the accuracy of all the information (the "Content") contained in the publications on our platform. However, Taylor & Francis, our agents, and our licensors make no representations or warranties whatsoever as to the accuracy, completeness, or suitability for any purpose of the Content. Any opinions and views expressed in this publication are the opinions and views of the authors, and are not the views of or endorsed by Taylor & Francis. The accuracy of the Content should not be relied upon and should be independently verified with primary sources of information. Taylor and Francis shall not be liable for any losses, actions, claims, proceedings, demands, costs, expenses, damages, and other liabilities whatsoever or howsoever caused arising directly or indirectly in connection with, in relation to or arising out of the use of the Content.

This article may be used for research, teaching, and private study purposes. Any substantial or systematic reproduction, redistribution, reselling, loan, sub-licensing, systematic supply, or distribution in any form to anyone is expressly forbidden. Terms & Conditions of access and use can be found at <http://www.tandfonline.com/page/terms-and-conditions>

Theta-gamma phase-phase coupling during working memory maintenance in the human hippocampus

Leila Chaieb¹, Marcin Leszczynski¹, Nikolai Axmacher^{2,3}, Marlene Höhne¹, Christian E. Elger^{1,4}, and Juergen Fell¹

¹Department of Epileptology, University of Bonn, Bonn, Germany

²Department of Neuropsychology, Institute of Cognitive Neuroscience, Ruhr-University Bochum, Bochum, Germany

³German Center for Neurodegenerative Diseases, Bonn, Germany

⁴Life and Brain GmbH, Bonn, Germany

The theta-gamma neural coding theory suggests that multiple items are represented in working memory (WM) by a superposition of gamma cycles on theta oscillations. To enable a stable, non-interfering representation of multiple items, such a theta-gamma neural code may be reflected by phase-phase coupling, i.e., a precise locking of gamma subcycles to specific theta phases. Recent data have indicated that the hippocampus critically contributes to multi-item working memory. Therefore, we investigated phase-phase coupling patterns in the hippocampus based on intracranial EEG recordings in presurgical epilepsy patients performing a variant of the serial Sternberg WM task. In accordance with predictions of the theta-gamma coding theory, we observed increased phase-phase coupling between theta and beta/gamma activity during working memory maintenance compared to inter-trial intervals. These phase-phase coupling patterns were apparent during maintenance of two and four items, but not during maintenance of a single item, where prominent lower coupling ratios occurred. Furthermore, we observed that load-dependent changes of coupling factors correlated with individual WM capacities. Our data demonstrate that multi-item WM is associated with changes in hippocampal phase-phase coupling between theta and beta/gamma activity.

Keywords: Working memory; Intracranial EEG; Hippocampus; n:m phase coupling; Theta activity; Gamma activity.

According to the theta-gamma coding model multiple items are represented in working memory (WM) by a nesting of gamma subcycles within theta oscillations (Jensen & Lisman, 2005; Lisman & Idiart, 1995; Lisman & Jensen, 2013). These gamma cycles are supposed to reflect the activity of different neural assemblies each representing a distinct item maintained in WM. It is therefore necessary, within

the framework of this model, that gamma cycles are precisely locked to specific phases of theta oscillations in order to enable a stable, non-interfering representation of multiple items. In other words, gamma and theta oscillations should be 1:m phase-phase coupled. For instance, a theta oscillation of 5 Hz and a gamma oscillation of 30 Hz may exhibit a 1:6 phase coupling. This means that gamma phases

Correspondence should be addressed to: Juergen Fell, Department of Epileptology, University of Bonn, Sigmund-Freud-Str. 25, D-53105 Bonn, Germany. E-mail: juergen.fell@ukb.uni-bonn.de

We would like to thank Dr. Hui Zhang for her programming advice and for her insightful comments concerning the WM paradigm.

There are no financial interests or benefits arising from direct applications of this research.

This work was supported by a grant from the German Research Foundation (project FE 366/6-1) and SFB 1089.

of 0° are, for example, locked to theta phases of 0° , 60° , 120° , 180° , 240° , and 300° . As representations of multiple items are probably separated by temporal gaps, maximal WM capacity should be well below the coupling factor m .

In practice, $1:m$ phase-phase coupling can be quantified by evaluating the distribution of phase differences between the phases of the lower frequency oscillation and m times the phases of the higher frequency oscillations, similar to the way in which phase synchronization is calculated (e.g., Tass et al., 1998). Findings based on surface EEG recordings in humans showed evidence of phase-phase coupling between parietal theta and gamma oscillations during WM maintenance (Sauseng et al., 2009). In accordance with the theta-gamma coding model, the load-dependent increases of theta-gamma phase-phase coupling predicted individual WM capacities.

Over the last decade, increasing evidence has suggested that the hippocampus is not only prominently involved in long-term memory, but also plays a critical role in multi-item WM processing (e.g., Axmacher et al., 2007; Piekema, Kessels, Mars, Petersson, & Fernández, 2006). Recently, phase-phase coupling between theta and gamma oscillations in the CA1 region of rat hippocampus during maze exploration has been reported (Belluscio, Mizuseki, Schmidt, Kempter, & Buzsaki, 2012). However, it is not yet known whether such phase-phase coupling exists in the human hippocampus, and if it is involved in multi-item WM. Here, we asked whether phase-phase coupling between theta and gamma oscillations occurs in the human hippocampus during multi-item WM maintenance, as predicted by the theta-gamma coding model. To test this hypothesis, we reanalyzed hippocampal recordings from presurgical epilepsy patients performing a serial Sternberg task under varying load conditions consisting of either one, two, or four items. In order to investigate WM for ecologically relevant novel material, for which processes in the hippocampus are particularly important (e.g., Stern, Sherman, Kirchoff, & Hasselmo, 2001), we used faces as stimuli.

METHODS

Subjects

Fourteen patients with pharmaco-resistant temporal lobe epilepsy participated in the study. In nine patients, unilateral hippocampal sclerosis was

confirmed histologically. In the others, one had a unilateral isolated amygdala lesion, two had no apparent MRI lesions, and two had unilaterally accentuated limbic pathologies. Recordings were performed from 2004 to 2007 at the Department of Epileptology, University of Bonn, Germany. Thirteen patients had bilateral hippocampal depth electrodes, and only electrode sites contralateral to the epileptogenic zone were considered. One patient had a single electrode in the right hippocampus and showed an extrahippocampal (temporo-occipital) seizure onset zone. No seizure occurred within 24 hours prior to the experiment. The study was approved by the local medical ethics committee of the University of Bonn, and all patients gave written informed consent. Due to a corrupted EEG file, data from one patient with unilateral hippocampal sclerosis could not be used, so that iEEG data from 13 patients were subjected to analysis (three women; mean age \pm S: 37.7 ± 11.6 years; 10 right handed).

Experimental paradigm

We used a modified version of the Sternberg paradigm with a serial presentation of items. The Sternberg paradigm allows for a parametric modulation of the WM load, i.e., the number of items that have to be maintained over a short interval (Figure 1). Subjects were required to memorize either one, two, or four black and white photographs of unknown male and female faces (total of 126 male and 126 female faces) that had previously been rated by a large group of subjects as being neutral with respect to facial expression (three-point scale). Each picture was presented in the center of a computer screen for 500 ms with a randomized interstimulus interval that had a mean of 1400 ms and a range of 1300–1500 ms. Afterwards, patients had to maintain the faces in WM for 3000 ms. Subsequently, patients were presented with a probe for 500 ms and had to decide whether it matched one of the faces seen during that trial's encoding phase ("target") or not ("non-target"). Half of the trials were target and non-target trials, respectively. The length of the inter-trial interval was 5000 ms. Faces were shown only within one trial and were not repeated during the experiment (108 trials were presented in total). Patients indicated their decision by pressing one of two buttons of a computer mouse with their dominant hand. The overall duration of the experiment was about 20 minutes. During the experiment, we recorded continuous EEG from the implanted depth electrodes as well as from bilateral mastoid electrodes. Only trials

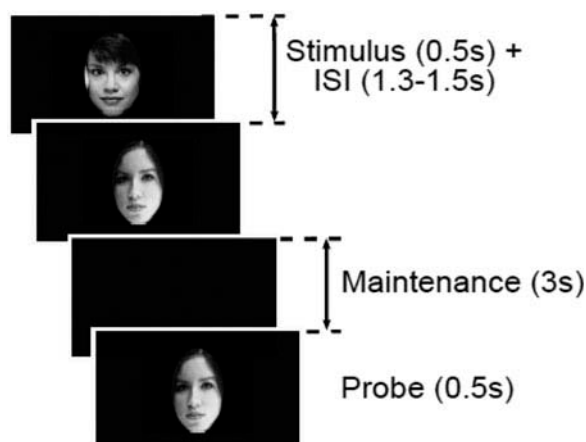


Figure 1. Overview of the modified Sternberg WM paradigm.

with correct responses were taken into account for the iEEG analyses.

iEEG recording and preprocessing

Multicontact depth electrodes were inserted for diagnostic purposes using a computer tomography-based stereotactic insertion technique (Van Roost, Solymosi, Schramm, Van Oosterwyck, & Elger, 1998). The location of electrode contacts was ascertained by obtaining an MRI for each patient and was classified as either hippocampal, rhinal, or other. On average, patients had 5.4 ± 1.9 hippocampal contacts (mean \pm *SD*). Depth EEG was referenced to linked mastoids, recorded at a sampling rate of 1000 Hz, and band-pass filtered (0.01 Hz (6 dB/octave) to 300 Hz (12 dB/octave)). For phase-phase coupling analysis we selected the hippocampal electrode contact from the contralateral side (i.e., contralateral to the seizure focus) in each patient, which showed the largest load-dependent changes of the DC potential slopes (i.e., the inclinations of linear regression lines fitted to the EEG), as this measure likely reflects WM maintenance (Axmacher et al., 2007). In the one patient with a unilateral depth electrode, the equivalent contact from that electrode was used, which was distant from the temporo-occipital seizure onset zone. EEG trials representing the maintenance intervals were segmented with regard to the onset of the last face stimulus [−1 s; 4.5 s] (i.e., interval ranging from 1 s before stimulus onset to 4.5 s after stimulus onset). EEG trials representing the inter-trial intervals were segmented with regard to the onset of the first face stimulus [−5.5 s; 0 s]. All

EEG trials were visually inspected for artifacts (e.g., epileptiform spikes, spike wave complexes, etc.), and 37% of all trials were excluded from the analysis. After artifact rejection across all patients, 334 maintenance trials remained for Load 1 (inter-trial intervals: 328), 332 trials for Load 2 (inter-trial intervals: 342), and 289 trials for Load 4 (inter-trial intervals: 290).

Phase-phase coupling analysis

All trials were filtered using second-order zero-phase Butterworth filters (MATLAB, R2013b) with a width of 1 Hz centered around the following frequencies: From 1 to 20 Hz in 1-Hz steps and these frequencies multiplied by the factors 2–8 (i.e., each low-frequency oscillation was paired with seven high-frequency oscillations). To avoid the influence of edge effects, the filtered trials were then trimmed [to 0 s; 3.5 s] for the maintenance intervals and [−4.5 s; −1 s] for the inter-trial intervals (Figure 2 displays an example of a filtered trial from Load 4). From the filtered trials phase values were extracted for each time point based on Hilbert transform. After that, 1:m phase coupling was evaluated for the factors $m = 2$ to $m = 8$ based on circular variance (e.g., Lachaux, Rodriguez, Martinerie, & Varela, 1999). In detail, phase differences between the low-frequency phases multiplied by the factor m and the high-frequency phases were calculated and transformed into complex vectors. For each trial, these complex vectors were averaged across maintenance and inter-trial intervals yielding trial-specific circular variance vectors. Then, for each subject these trial-specific vectors were averaged across trials, across all

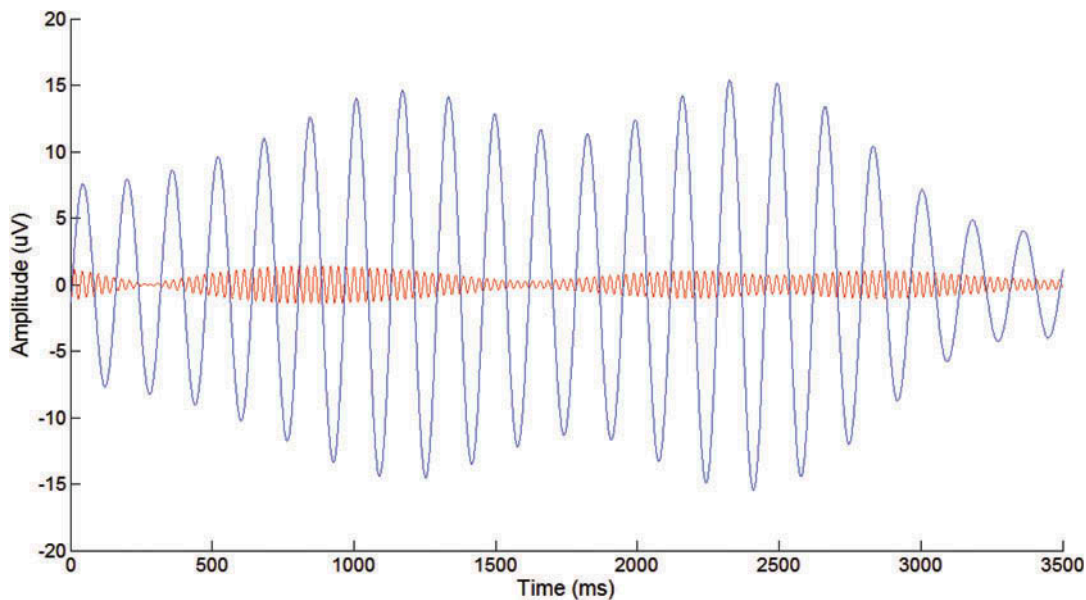


Figure 2. Example of a filtered EEG trial at WM load 4. Butterworth-filtered EEG trial from one patient at 6 Hz (blue curve) and 36 Hz (red curve).

maintenance intervals, and across all inter-trial intervals. Trial-specific vectors were also averaged across the maintenance intervals independently for WM Loads 1, 2, and 4. Finally, the 1:m phase coupling values were extracted from the norm of these average circular variance vectors.

Non-parametric statistical analysis

Statistical evaluation was based on non-parametric label-permutation tests (Maris & Oostenveld, 2007). We compared average phase-phase coupling values during the maintenance intervals for Loads 1, 2, 4, and for all (without load split) items with average phase-phase coupling values for all inter-trial intervals. In a first step, differences between these conditions (maintenance of 1, 2, 4, all vs. inter-trial interval) across subjects were explored using paired *t*-tests. In a second step, those frequency-frequency combinations with significant *t*-test results ($p < .05$) were subjected to a label-permutation test. For this purpose, condition labels (maintenance and inter-trial) were randomly permuted 1000 times across subjects, and *t*-values were again calculated on the basis of paired *t*-tests for each permutation. Then, the *t*-value for the original comparison was ranked among the *t*-values resulting from random label permutation, which yielded the final significance value.

Correlation between WM capacities and phase-phase coupling factors

We calculated inter-individual correlations between WM capacities and changes of phase-phase coupling factors m across memory loads (for a similar approach, see Sauseng et al., 2009). For each subject the relative coupling factor (difference between maintenance and load-specific inter-trial intervals) at the maximum coupling strength was extracted for WM loads two and four (within the frequency range: 1–10 Hz). Capacity was estimated with Cowan's k (Cowan, 2001; Rouder, Morey, Morey, & Cowan, 2011) and calculated for each participant and each load condition by means of hit rate (probability of matched probes to be correctly identified as “old”), false alarm rate (probability of non-matched probes to be wrongly classified as “old”), and WM load (number of to be maintained items):

$$k = (\text{hit rate} - \text{false alarm rate}) * \text{WM load}$$

Subsequently, for each participant the maximum value of k across WM loads (k_{\max}) was used in the correlation analysis. The association between WM capacity k_{\max} and the coupling factor difference (coupling factor load 4—coupling factor load 2) was quantified with Kendall's tau rank correlation. The

rationale for this analysis is that, based on the theta-gamma coding model, subjects with low WM capacity would be expected to show a smaller load-dependent increase of coupling factors than subjects with high WM capacity.

RESULTS

The significance values of phase-phase coupling increases and decreases during the maintenance intervals across all WM loads compared to the inter-trial intervals are shown in Figure 3 panel A (see Figure 4, panels A–D for corresponding relative percentage changes). As hypothesized, the most prominent WM-related phase-phase coupling increases occur between theta oscillations at 3 and 6 Hz and beta/gamma oscillations at 18 and 36 Hz, i.e., with a coupling factor of 6. Interestingly, the phase-phase coupling increase at 3 Hz is flanked by a prominent phase-phase coupling decrease at 4 Hz with the same coupling factor of 6.

The findings for the individual WM load conditions (Figure 3, panels B, C, and D) indicate that the phase-phase coupling increases with a coupling factor of 6 were not apparent for a WM load of one item. Here, the pattern of phase-phase coupling increases is dominated by couplings with lower factors, in particular, couplings between 3 and 6 Hz (factor 2; increase of 8.7%; $p = .006$) and between 7 and 35 Hz (factor 5; increase of 7.6%; $p = .019$). For a WM load of two items, a phase-phase coupling increase between 6 Hz and 36 Hz was detected (factor 6; 7.3%; $p = .009$), while coupling effects with lower factors, that were observed for a load of one item, disappear. This finding suggests that higher WM loads are accompanied by changes of higher phase-phase coupling factors, while lower WM loads correspond to changes of lower factors.

For a WM load of four items, the phase-phase coupling pattern at a factor of 6 described above becomes apparent, with coupling increases at 3 Hz (9.3%; $p = .005$) and 6 Hz (8.5%; $p = .008$), and a decrease at 4 Hz (−10.4%; $p = .001$). Apart from this

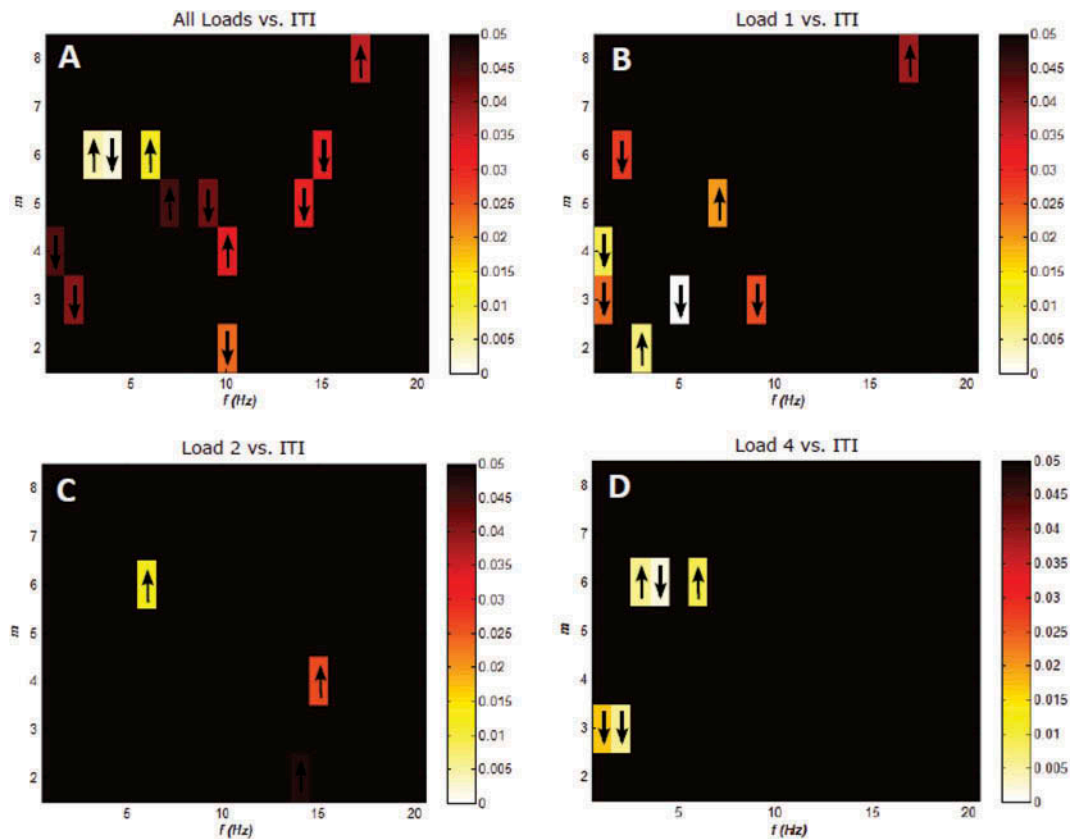


Figure 3. Phase-phase coupling results (significance values). Panel A: Statistical significances of phase-phase coupling changes during the maintenance intervals across all load conditions vs. inter-trial intervals (upward arrows indicate phase-phase coupling increases; downward arrows indicate phase-phase coupling decreases). Panels B, C, and D: Statistical significances of phase-phase coupling changes during the maintenance intervals for a WM load of one, two, and four items vs. inter-trial intervals.

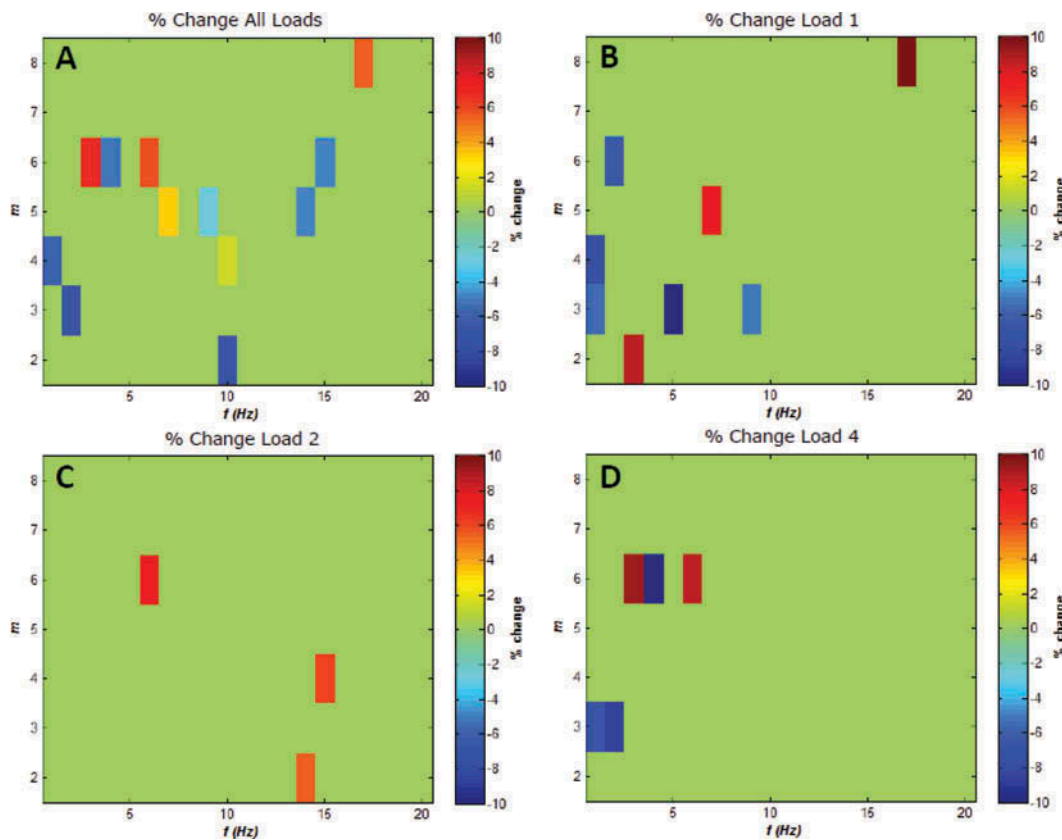


Figure 4. Phase-phase coupling results (percentage change). Panel A: Statistically significant phase-phase coupling changes (%) during the maintenance intervals across all load conditions vs. inter-trial intervals. Panels B, C, and D: Statistically significant phase-phase coupling changes (%) during the maintenance intervals for a WM load of one, two, and four items vs. inter-trial intervals.

pattern, only phase-phase coupling decreases are evident for a load of four items, between 1 Hz and 3 Hz (factor 3; -6.7% ; $p = .009$) and between 2 Hz and 6 Hz (factor 3; -8.5% ; $p = .005$). Interestingly, the upper frequencies of these phase-phase coupling decreases again appear as lower frequencies for the 3 Hz versus 18 Hz (factor 6) and 6 Hz versus 36 Hz (factor 6) phase-phase coupling increases.

One may wonder whether the reported phase-phase coupling effects may be generated by spectral power increases (decreases) via improvement (deterioration) of the signal to noise ratio. To check for this possible bias, we calculated spectral power (using a similar analysis approach as for the extraction of phases, i.e., extraction of squared amplitudes after Butterworth filtering and Hilbert transform) for the frequencies where we found the major phase-phase coupling effects, i.e., for theta frequencies between 3 and 7 Hz and gamma frequencies at a factor of 6 (i.e., for 3, 4, 5, 6, 7, 18, 24, 30, 36, 42 Hz). We only found decreases in spectral power during maintenance versus inter-trial intervals: During Load 1 at 36 Hz ($p = .047$), during

Load 2 at 18 Hz ($p = .037$), and during Load 4 at 7 Hz ($p = .039$). Phase-phase coupling effects were not observed for any of these frequencies and load conditions, thus ruling out an influence of power changes on the major phase-phase coupling results.

The theta-gamma coding model implies that the number of gamma cycles locked to theta oscillation represents a limit for the number of items that can be maintained in WM. In particular, the increase of the coupling factor m across memory loads may predict individual WM capacity. To test this prediction, we calculated Kendall's tau rank correlation between individual WM capacities (k_{\max}) and the differences of coupling factors m with maximal coupling strength between a WM load of four items and load of two items. We observed a significant positive correlation between WM capacities and coupling factor changes ($\text{tau} = 0.59$, $p = .009$), suggesting that patients with greater increases of coupling factors are able to maintain more items in WM (see Figure 5). When selecting the differences of coupling factors at the minimal coupling strengths (i.e., at the phase-phase coupling

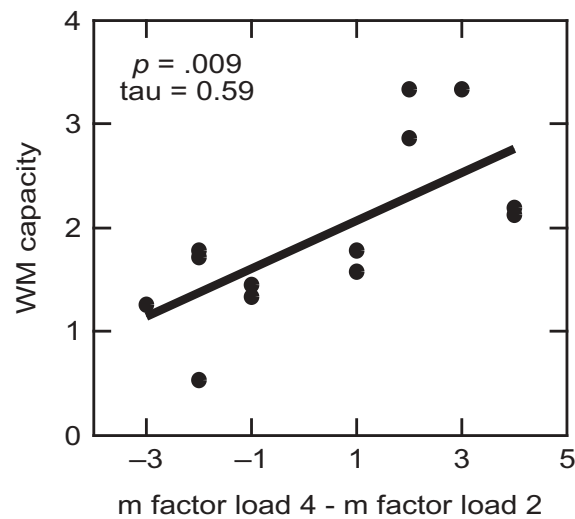


Figure 5. Relation of phase-phase coupling to behavior. The amount of coupling factor increase predicts individual WM capacity as indicated by a positive correlation. Each dot represents individual subjects.

decreases), we found no significant correlation with individual working memory capacities.

We would like to emphasize that, in the absence of empirical data for the human hippocampus, the phase-phase coupling findings depicted in Figures 2 and 3 represent results of a broad, exploratory analysis approach. Permutation-based cluster approaches are not applicable for these data, since the effects do not extend across several frequency-frequency pairs. When we perform a strict Bonferroni correction based on our hypothesis of theta versus beta/gamma phase-phase coupling (theta 3–7 Hz, factors 2–8: Adjustment value: $5 \times 7 = 35$), only WM-related phase-phase coupling decreases are statistically significant under the corrected threshold of $p = .0014$. These are the decreases of phase-phase coupling between 4 and 24 Hz (factor 6) across all load conditions ($p = .001$) and for Load 4 ($p = .001$), as well as the decrease of phase-phase coupling between 5 and 15 Hz (factor 3) for Load 1 ($p < .001$).

GENERAL DISCUSSION

The present study is the first to demonstrate phase-phase coupling in the human hippocampus during multi-item WM maintenance. Previous studies have described phase-phase coupling during WM processing in humans based on non-invasive recordings. Surface EEG data have suggested phase-phase coupling during WM maintenance between frontal theta oscillations and centroparietal alpha oscillations (Schack, Klimesch, & Sauseng, 2005), and between parietal theta and

gamma oscillations (Sauseng et al., 2009). In the latter study, the load-dependent increase of theta–upper gamma phase-phase coupling during WM maintenance predicted individual working memory capacity (Sauseng et al., 2009). Furthermore, based on magnetoencephalography data, a WM load-dependent enhancement of alpha–gamma phase-phase coupling during an arithmetic task has also been reported (Palva, Palva, & Kaila, 2005).

According to the relational memory theory (e.g., Cohen & Eichenbaum, 1993; Henke, 2010), WM processes involving multiple items or associations of multiple-item features are not only facilitated by neocortical regions, but are also crucially supported by the hippocampus. Indeed, experimental evidence has accumulated during recent years supporting a role of the hippocampus in multiple-item and relational WM (see, e.g., Fell & Axmacher, 2011). However, phase-phase coupling in the human hippocampus during WM processing had not yet been reported.

In the present investigation, we observed prominent changes of phase-phase coupling during WM maintenance compared to inter-trial intervals, under load conditions of two and four, in particular between theta and beta/gamma oscillations with a coupling factor of 6. Such concomitant coupling is in accordance with the predictions of an influential model suggesting that multiple items are coded in WM by gamma subcycles nested in theta oscillations (Jensen & Lisman, 2005; Lisman & Idiart, 1995; Lisman & Jensen, 2013). In the framework of this model, a phase-phase coupling factor of 6 for face stimuli would correspond to a maximal WM capacity of well below 6 (as there are most likely temporal gaps between the representations

of series of items to avoid interference), which is in agreement with empirical findings, suggesting a typical WM capacity limit of around four items (Cowan, 2001).

In a previous study investigating phase-amplitude coupling in the same data set, we also found increased coupling between theta and beta/gamma activity during WM maintenance compared to inter-trial intervals (Axmacher et al., 2010). Coupling factors for WM-related phase-amplitude coupling ranged from 2–7 with a peak value around 4. Thus, the coupling factor of 6 observed for WM-related phase-phase coupling in the present study is at the upper end of the coupling factor range previously observed for phase-amplitude coupling. It has been suggested that phase-amplitude coupling represents a coarse mechanism modulating beta/gamma activity in a broad frequency and time range, while phase-phase coupling enables a more temporally fine-tuned and frequency-specific modulation (Fell & Axmacher, 2011). This idea is supported by our observation of WM-related increases of phase-phase coupling only for specific frequency-frequency pairs and not for the neighboring pairs. Interestingly, we found for phase-amplitude coupling that the variance across trials of coupling phases (i.e., theta phases where beta/gamma activity is maximal) decreased with memory load (Axmacher et al., 2010). This finding is in line with the WM-related increases of phase-phase coupling between theta and beta/gamma activity for higher loads observed in the present study.

Nevertheless, the most significant effects detected in the present investigation were phase-phase coupling decreases. Under the highest WM load the phase-phase coupling increase at 3 Hz (factor 6) was flanked by a decrease at 4 Hz (factor 6). This finding again suggests that phase-phase coupling effects are more fine-tuned and frequency-specific than phase-amplitude coupling effects, which were broadly extended in the frequency-frequency space (Axmacher et al., 2010). In the context of the theta-gamma coding model (Jensen & Lisman, 2005; Lisman & Idiart, 1995; Lisman & Jensen, 2013), frequency-frequency pairs exhibiting phase-phase coupling decreases would not be suited for the coding of WM items, as the timing of beta/gamma cycles across theta oscillations and therefore the temporal representations of WM items is not stable. In this sense, such frequency-frequency pairs are possibly disabled for phase-phase coding. Furthermore, the upper frequencies of phase-phase coupling decreases at 1 and 3 Hz (both factor 3) again appeared as lower frequencies for the increases at 3 and 6 Hz (both factor 6). One may

speculate that both effects possibly result in a dampening of irrelevant couplings, in favor of a sharpening and tuning of the relevant phase-phase coupling increases at 3 and 6 Hz.

Most importantly, we observed a positive correlation between individual WM capacities and the changes of coupling factors from Load 2 to Load 4 at the maximal phase-phase coupling increases. In the framework of the theta-gamma coding model (Jensen & Lisman, 2005; Lisman & Idiart, 1995; Lisman & Jensen, 2013), phase-phase coupling factors represent an upper limit for the number of items that can be maintained in WM. Accordingly, subjects with higher working memory capacities are expected to show larger load-dependent increases of phase-phase coupling factors. Hence, this result is in agreement with the predictions of the theta-gamma coding model and it is in line with the outcome of a previous surface EEG study (Sauseng et al., 2009). To summarize, our findings demonstrate that hippocampal phase-phase coupling patterns are modulated by WM load and are correlated with WM performance.

Original manuscript received 19 March 2015

Revised manuscript received 29 May 2015

First published online 26 June 2015

REFERENCES

- Axmacher, N., Henseler, M. M., Jensen, O., Weinreich, I., Elger, C. E., & Fell, J. (2010). Cross-frequency coupling supports multi-item working memory in the human hippocampus. *Proceedings of the National Academy of Sciences*, *107*, 3228–3233. doi:10.1073/pnas.0911531107
- Axmacher, N., Mormann, F., Fernandez, G., Cohen, M. X., Elger, C. E., & Fell, J. (2007). Sustained neural activity patterns during working memory in the human medial temporal lobe. *Journal of Neuroscience*, *27*, 7807–7816. doi:10.1523/JNEUROSCI.0962-07.2007
- Belluscio, M. A., Mizuseki, K., Schmidt, R., Kempster, R., & Buzsaki, G. (2012). Cross-frequency phase-phase coupling between theta and gamma oscillations in the hippocampus. *Journal of Neuroscience*, *32*, 423–435. doi:10.1523/JNEUROSCI.4122-11.2012
- Cohen, N. J., & Eichenbaum, H. (1993). *Memory, amnesia, and the hippocampal system*. Cambridge, MA: The MIT Press.
- Cowan, N. (2001). The magical number 4 in short-term memory: A reconsideration of mental storage capacity. *Behavioral Brain Sciences*, *24*, 87–114. doi:10.1017/S0140525X01003922
- Fell, J., & Axmacher, N. (2011). The role of phase synchronization in memory processes. *Nature Reviews Neuroscience*, *12*, 105–118. doi:10.1038/nrn2979
- Henke, K. (2010). A model for memory systems based on processing modes rather than consciousness. *Nature*

- Reviews Neuroscience*, 11, 523–532. doi:10.1038/nrn2850
- Jensen, O., & Lisman, J. E. (2005). Hippocampal sequence-encoding driven by a cortical multi-item working memory buffer. *Trends in Neurosciences*, 28, 67–72. doi:10.1016/j.tins.2004.12.001
- Lachaux, J. P., Rodriguez, E., Martinerie, J., & Varela, F. J. (1999). Measuring phase synchrony in brain signals. *Human Brain Mapping*, 8, 194–208. doi:10.1002/(SICI)1097-0193(1999)8:4<194::AID-HBM4>3.0.CO;2-C
- Lisman, J. E., & Idiart, M. A. (1995). Storage of 7 ± 2 short-term memories in oscillatory subcycles. *Science*, 267, 1512–1515. doi:10.1126/science.7878473
- Lisman, J. E., & Jensen, O. (2013). The theta-gamma neural code. *Neuron*, 77, 1002–1016. doi:10.1016/j.neuron.2013.03.007
- MATLAB ??(?.?) [Computer software]. http://uk.mathworks.com/products/matlab/?s_tid=hp_fp_ml
- Maris, E., & Oostenveld, R. (2007). Nonparametric statistical testing of EEG- and MEG-data. *Journal of Neuroscience Methods*, 164, 177–190. doi:10.1016/j.jneumeth.2007.03.024
- Palva, J. M., Palva, S., & Kaila, K. (2005). Phase synchrony among neuronal oscillations in the human cortex. *Journal of Neuroscience*, 25, 3962–3972. doi:10.1523/JNEUROSCI.4250-04.2005
- Piekema, C., Kessels, R. P. C., Mars, R. B., Petersson, K. M., & Fernández, G. (2006). The right hippocampus participates in short-term memory maintenance of object-location associations. *Neuroimage*, 33, 374–382. doi:10.1016/j.neuroimage.2006.06.035
- Rouder, J. N., Morey, R. D., Morey, C. C., & Cowan, N. (2011). How to measure working memory capacity in the change detection paradigm. *Psychonomic Bulletin & Review*, 18, 324–330. doi:10.3758/s13423-011-0055-3
- Sauseng, P., Klimesch, W., Heise, K. F., Gruber, W. R., Holz, E., Karim, A. A. ... Hummel, F. C. (2009). Brain oscillatory substrates of visual short-term memory capacity. *Current Biology*, 19, 1846–1852. doi:10.1016/j.cub.2009.08.062
- Schack, B., Klimesch, W., & Sauseng, P. (2005). Phase synchronization between theta and upper alpha oscillations in a working memory task. *International Journal of Psychophysiology*, 57, 105–114. doi:10.1016/j.ijpsycho.2005.03.016
- Stern, C. E., Sherman, S. J., Kirchoff, B. A., & Hasselmo, M. E. (2001). Medial temporal and prefrontal contributions to working memory tasks with novel and familiar stimuli. *Hippocampus*, 11, 337–346. doi:10.1002/(ISSN)1098-1063
- Tass, P., Rosenblum, M. G., Weule, J., Kurths, J., Pikovsky, A., Volkman, J. ... Freund, H.-J. (1998). Detection of n:m phase locking from noisy data: Application to magnetencephalography. *Physical Review Letters*, 81, 3291–3294. doi:10.1103/PhysRevLett.81.3291
- Van Roost, D., Solymosi, L., Schramm, J., Van Oosterwyck, B., & Elger, C. E. (1998). Depth electrode implantation in the length axis of the hippocampus for the presurgical evaluation of medial temporal lobe epilepsy: A computed tomography-based stereotactic insertion technique and its accuracy. *Neurosurgery*, 43, 819–826. doi:10.1097/00006123-199810000-00058